

# Seasonally Different Response of the Indian Ocean to the Remote Forcing of El Niño: Linking the Dynamics and Thermodynamics

Masamichi Ohba<sup>1</sup> and Hiroaki Ueda<sup>2</sup>

<sup>1</sup>Central Research Institute of Electric Power Industry, Abiko, Japan

<sup>2</sup>Graduate School of Life and Environmental Sciences, University of Tsukuba, Tsukuba, Japan

## Abstract

Physical processes involved in basin-wide warming (BW) in the Indian Ocean (IO) and the IO “Dipole” mode (IOD) are investigated, using solutions to an air-sea coupled general circulation model (CGCM). In this study, we pay attention to the seasonal difference of the IO SST in response to the ENSO. A suite of time-slice CGCM experiments, by imposing the El Niño-related SST anomalies in the Pacific for the boreal summer and fall, are conducted to study the El Niño impact on the IO SST anomalies. The impacts of El Niño largely depend on the monsoon seasonality, and significantly contribute to the IOD and IO BW. Additional experiments demonstrate the salient seasonal difference in the SST sensitivity to the ocean dynamics.

## 1. Introduction

In comparison with the large fluctuations in sea surface temperature (SST) in the tropical Pacific during El Niño-Southern Oscillation (ENSO), interannual SST variations in the Indian Ocean (IO) are rather modest. It is now widely recognized that the dominant interannual variability of the IO SST is basin-wide warming (BW), which lags a few months behind the mature phase of El Niño (e.g., Klein et al. 1999). Recently, studies on the influence of the second dominant SST variations have expanded considerably, in part due to the debate about the Indian Ocean “Dipole” mode (IOD), a mode of climate variability associated with cooling in the equatorial eastern Indian Ocean (EEIO) and warming in the western basin during boreal fall (Saji et al. 1999; Webster et al. 1999; Murtugudde and Busalacchi 1999). The IOD has two aspects of theory that the events are air-sea coupled mode internal to the IO itself (e.g., Yamagata et al. 2003) or forced by ENSO (e.g., Xie et al. 2002; Annamalai et al. 2003; Li et al. 2003) because of the high simultaneous correlation between the IOD and Niño-3.4 SST anomalies (SSTA) during boreal fall (Allan et al. 2001). Recently, some papers show the importance of the IO SST variation on the ENSO system (e.g., Kug and Kang 2006) especially on its strength (Annamalai et al. 2005) and transition (Ohba and Ueda 2007). Despite its importance in understanding the physical interaction of the air-sea coupled system between the IO and Pacific, both the ENSO-dependent and intrinsic mechanisms are not completely clear and still under discussion.

Observational studies have suggested that the IOD could be triggered by El Niño-related reversed Walker circulation (RWC) over the tropical IO, through the modulation of monsoon base flow over the IO (e.g., Ueda and Matsumoto 2000; Lau and Nath 2004). Li et al.

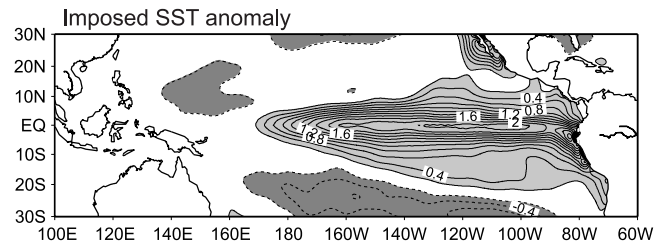


Fig. 1. Imposed SSTA (°C) in the CGCM time-slice experiments. The SSTA are obtained from the composite of observed El Niño.

(2003) pointed out the importance of the monsoon seasonality and controlled mean flow to the generation of the IOD. Due to strong negative air-sea feedbacks in the northern winter, the IOD could not survive after boreal winter. However, specific factors and physical processes that give rise to the different SST pattern in different seasons is not complementary clear. To overcome this, we conducted a set of experiments using a stand-alone air-sea coupled general circulation model (CGCM) and caught a strong seasonality in the influence of El Niño on the tropical IO. The experiments are also expected to reveal the effect of the coupling process between El Niño forcing and monsoon base flow on the IO, and its seasonal difference. The paper is organized as follows. Section 2 presents a brief description of the CGCM. Section 3 examines the response of the IO in the CGCM to a heating source in the Pacific. Section 4 summarizes our conclusions.

## 2. Model

The model we use is MRI-CGCM2.3.2b, the air-sea coupled model developed by Meteorological Research Institute in Japan (Yukimoto et al. 2006). The model consists of an atmospheric general circulation model (AGCM) coupled with an oceanic general circulation model (OGCM). The AGCM is a global spectral model, which we ran at T42 resolution and with 30 sigma-pressure coordinate levels in the vertical. The oceanic component of the model is a Bryan-Cox type OGCM with a global domain. The horizontal grid spacing is 2.5 degrees in longitude and 2 degrees in latitude. Near the equator, between 4°S and 4°N, the meridional grid spacing is set to 0.5 degrees in order to provide good resolution of equatorial oceanic waves. In comparison with the tropical IO variability in the IPCC 20th-century climate simulations, the long-term CGCM simulation well reproduces observational temporal-spatial structure of both BW and IOD which show a strong correlation with those of the ENSO event (Saji et al. 2006). The simulated SST pattern in relation to the ENSO activity in the tropical Pacific is similar to what is typically observed (Yukimoto and Kitamura 2003), with a somewhat higher frequency.

Corresponding author: Masamichi Ohba, Central Research Institute of Electric Power Industry, Environmental Science Research Laboratory, 1646 Abiko, Abiko-shi, Chiba, 270-1194, Japan. E-mail: oba-m@criepi.denken.or.jp. ©2009, the Meteorological Society of Japan.

Table 1. A brief description of each of the time-slice CGCM experiments performed for this study. The same SSTA forcing is used, but the initial month for SR and FR is different. The experimental design represents the seasonality in the influences of El Niño.

IO	season	SR (Initial: Jul)	FR (Initial: Oct)
	coupled		SR
decoupled		DC-SR	DC-FR
only heat flux		HF-SR	HF-FR
only wind stress		WS-SR	WS-FR

### 3. Solutions to the CGCM

#### 3.1 Experimental design

Previous observational studies (e.g., Allan et al. 2001) revealed that the appearance of the IOD and BW in the IO depends on the season. The IOD and the BW in the IO could be forced by SSTA in the equatorial eastern Pacific via atmospheric teleconnection (Lau and Nath 2004; Shinoda et al. 2004). Ueda and Matsumoto (2000), using observational and reanalysis data, have suggested that the influence of El Niño on the underlying SST exhibit distinct seasonal difference. The RWC forced by the major El Niño episodes in the boreal summer and fall modulates the surface wind over the IO. The resulting wind speed changes in boreal summer (fall) cause the IOD (BW) in the succeeding fall (winter) through a modulation of the evaporative cooling and turbulent mixing of the underlying water. Therefore, the question we will address in this study is whether those SSTA are actually due to the remote impact of El Niño and how the monsoon seasonality of the atmospheric/oceanic flow are related to these processes.

Eight time-slice sensitivity experiments, divided into four groups, are conducted that are designed to yield a straightforward answer to the question. In the summer runs (SR), composited SSTA associated with El Niño are imposed in the tropical Pacific for July (Fig. 1). The SSTA is specified in the Pacific sector for the following three months and the coupling is maintained in the other regions. The composited SST is extracted from the most prominent El Niño episodes (1957, 65, 72, 82, 91 and 97) in the extended reconstructed SST version 2 (Smith and Reynolds 2004), averaged in 6-months during October to following March. The fall runs (FR) are similar to the SR, except that the SSTA are inserted for October. We use the climatological values for all other initial conditions in SR and FR except the Pacific. These experimental setups imply that the set of SR is assuming the early-onset type event such as 1972, 82 and 97 El Niño (Horii and Hanawa 2004). The climatology is obtained from 75-year mean of the CGCM control run. The control run represented here is a simulation for a control climate state with no anomalous forcing.

To specify the physical factors that are responsible for the SSTA, we conduct wind stress (WS) run and heat flux (HF) run by respectively using the climatological heat-flux and wind-stress each forcing scenarios. In these experiments, we specify surface fluxes with the model climatology in the IO but keep the air-sea coupling. This experimental design mainly aims to illustrate relative importance of dynamic and thermodynamic processes in regulating the IO SSTA. We also conduct air-sea decoupled (DC) run with specified climatological SST for each forcing scenarios. This experiment reveals how the atmospheric seasonal mean states affect the El Niño tele-connection patterns.

To only extract the impact of SSTA in the Pacific, we also conducted climatological Pacific SSTA run by use of the same initial conditions. The anomalies presented in the next sections are obtained by the differ-

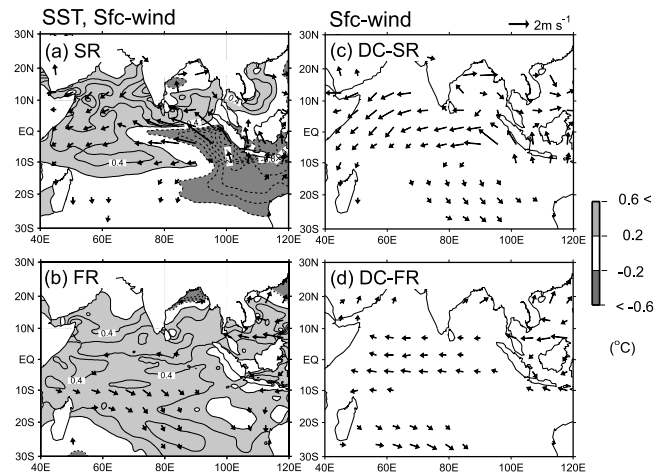


Fig. 2. Simulated SSTA in the September from (a) SR and (c) DC-SR, and December from (b) FR and (d) DC-FR. Shading denote the SSTA. Surface wind vector anomalies are plotted during the (a, c) JAS from SR and (b, d) OND from FR.

ence from the run. Thus, the SSTA obtained from this experiment mainly depends on the anomalous Pacific SST. To avoid the generation of the anomalous gravity waves in response to the sudden input of the El Niño, the atmospheric initial conditions are spun up for one month with prescribed Pacific SSTA. Thus, we analyzed the 3-months from the 4-month computation from the input of the Pacific SSTA. To account for the atmospheric sensitivity to the initial conditions, a 10-member ensemble approach is conducted. We changed only in the initial conditions, June 1 and September 1, selected from the CGCM control run in preserving the same SST forcing. Above experiments are summarized in Table 1.

#### 3.2 Effect of El Niño on the Indian Ocean SST

First, we show the composite anomalies of the simulated SSTA in the tropical IO, which will shed light on the remote impact of Pacific SSTA that can be directly compared between the SR and FR. Figure 2 shows the SSTA for the SR and DC-SR experiments, on the 3-months after inserting the composite SSTA. We superimpose the 3-month average of 850-hPa wind anomalies for the respective experiment. The SR generates zonally asymmetric SSTA, warm SSTA in the western basin and cold SSTA in the EEIO (Fig. 2a) with strong surface equatorial easterly. The spatial pattern of the SSTA and surface wind anomalies closely resembles the characteristics in the IOD (e.g., Saji et al. 1999). This relationship between the equatorial easterly anomalies and ENSO is also clearly seen in the observational study (Nagura and Konda 2005). Of particular interest is the strong anomalous equatorial easterly in the DC-SR (Fig. 2c), which is suggesting that the eastern Pacific SST could affect the zonal wind on the opposite side of the earth. The distribution of wind anomalies is similar to each other, without apparent difference in its intensity. The SST response in the series of FR (Fig. 2b) differs considerably from those in the SR. In the FR, as a direct response to the El Niño, basin-wide positive SSTA emerges in the tropical IO with weak easterly anomalies in the equatorial IO (Fig. 2b). SST observations from various sources indicate that the BW usually occurs during boreal winter and spring after the mature phase of El Niño (e.g., Klein et al. 1999).

Comparing the wind patterns in the SR and DC-SR, one may note that in addition to the remote SSTA impact, the IO SSTA has a local effect on the circulation anomaly in the region, especially modulation of the equatorial zonal wind anomalies (Figs. 2a and 2c). The

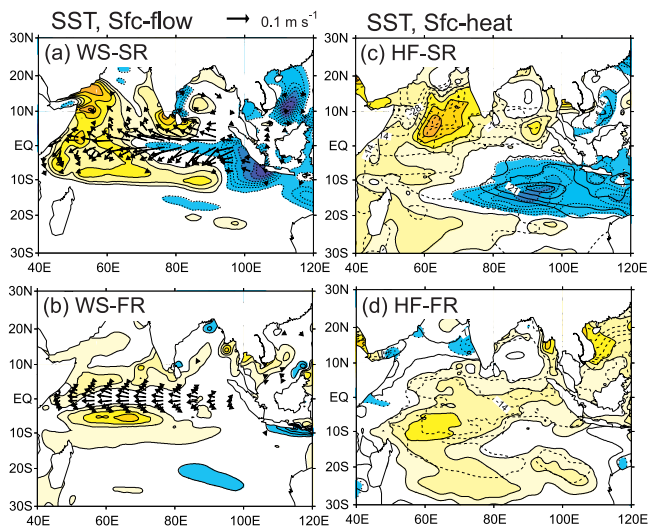


Fig. 3. Simulated SSTA in the September from (a) WS-SR and (c) HF-SR, and December from (b) WS-FR and (d) HF-FR. Contour interval is 0.2 ( $-0.2$ )  $^{\circ}\text{C}$ . Red (blue) shadings denote SSTA greater (less) than 0.2 ( $-0.2$ )  $^{\circ}\text{C}$ . Surface ocean current vector anomalies are superimposed during the (a) JAS from WS-SR and (b) OND from WS-FR. Surface heat-flux anomalies are represented in thick contour during the (c) JAS from HF-SR and (d) OND from HF-FR.

simulated zonal wind anomalies in SR and DC-SR have different peak positions, which might be attributed to the annual cycle of basic-state convective activities over the maritime continents. In boreal summer, the zonal wind anomalies are quite sensitive to external forcing over the EEIO at which seasonal convection is located. The local air-sea interaction in the SR strengthens the zonal wind anomalies around  $90^{\circ}\text{E}$ , suggesting the additional enhancement of the remote El Niño forcing. The comparison of the zonal wind anomalies in the fall between the couple and decoupled run illustrate that the local air-sea interaction decreases the atmospheric responses, as the ITCZ activities could be enhanced by the IO BW during the season. It is worth note that the intensities of the easterly anomalies for the decoupled experiments are significantly different between the boreal summer (DC-SR) and fall (DC-FR).

Figure 3 shows the simulated SSTA in the WS and HF run, on the 3-months after inserting the composited Pacific SSTA. We superimpose the 3-month average of the oceanic current averaged from surface to 50m-depth (Figs. 3a and 3c) and surface heat-flux (Figs. 3b and 3d) for the respective experiment. Of particular interest is that the WS-SR exhibiting the strong zonal gradient of SSTA (Fig. 3a) while slightly differs from the distribution in the SR (Fig. 2a). The anomalous easterly over the equatorial IO can excite oceanic Rossby and Kelvin waves along the thermocline. The Kelvin responses meet the surface in the EEIO and could enhance the oceanic upwelling, which may result in the constructed zonal SST contrast over the region (Webster et al. 1999).

The ENSO-induced RWC co-occurred with large-scale changes in surface wind speed over the basin. This is expected to contribute to the increase (decrease) in SST through a reduction (intensification) of vertical mixing in the ocean subsurface layer and heat exchange at the surface. It is interesting to note that the HF-SR (Fig. 3c) also induce the zonal SST contrast, though the result is relatively strong in comparison with the observation (e.g., Murtugudde and Busalacchi 1999). The comparison between the wind pattern in the SR (Fig. 2a) and surface heat-flux in the HF-SR (Fig. 3c) indicates that the easterly wind anomalies in the eastern

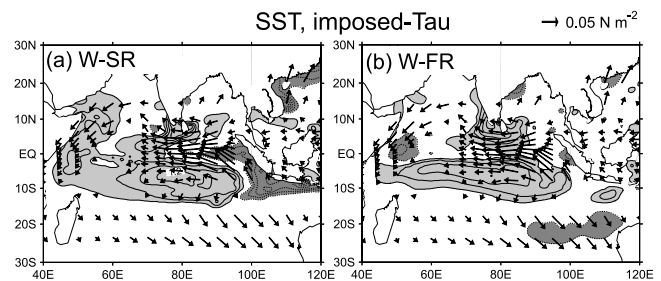


Fig. 4. Imposed wind stress anomalies ( $\text{N m}^{-2}$ ) and resultant SSTA in the (a) September for the W-SR and (b) December for the W-FR. The results are obtained from the OGCM time-slice experiments.

(western) part of the basin during boreal summer intensify (weaken) the climatological easterlies (westerlies) and induce the cooling (warming) through the enhancement (reduction) of evaporative cooling beyond the radiative damping (Ueda and Matsumoto 2000).

This result is consistent with the diagnosis of OGCM response to observed surface forcing (Li et al. 2002). The results of these experiments indicate that the modulations of both thermodynamics and ocean dynamics possibly construct the zonally asymmetric SSTA through the air-sea coupled system. Thus, both atmospheric and oceanic mean state produce the seasonal dependent air-sea coupled instability in this season. The easterly anomalies in response to the remote Pacific SSTA during boreal summer possibly cause the zonal SST gradient over the IO through the response of ocean dynamic and thermodynamic processes, and the SST change in turn can strengthen the equatorial easterlies.

Unlike in the case of WS-SR, the SST response in the WS-FR only reveals the Rossby response at north and south western IO (Fig. 3b). It is interesting to note that the cold SSTA off the coast of Sumatra could not be seen. The SST response of the HF-FR (Fig. 3d) reveals a significant warming of the central IO corresponding to the reduced surface heat-flux at the ocean surface. The El Niño-related easterly anomalies in the HF-FR weaken the heat exchange at the central IO. The surface wind anomalies in response to the Pacific SST forcing play a significant role to warm the SST in the central IO through the reduced heat exchange at the surface. The anomalous heating over the surface tropical IO ( $50^{\circ}\text{E}$ – $100^{\circ}\text{E}$ ,  $10^{\circ}\text{S}$ – $10^{\circ}\text{N}$ , 50 m) in the WS-FR (Fig. 3b) is  $2.4 \times 10^7 \text{ J m}^{-2}$ , whereas those of the HF-FR (Fig. 3d) is  $4.7 \times 10^7 \text{ J m}^{-2}$ . The IO BW is mainly induced by the anomalous surface heat-flux, while the impact of oceanic waves to the ocean surface is influential in the western part of the basin. The results obtained from these experiments are consistent with the observational studies (e.g., Xie et al. 2002).

The most conspicuous feature in the HF run is the difference in oceanic upwelling of cold water off the coast of Sumatra. The upwelling is largely caused by the combination of equatorial Kelvin wave and local enhancement of the upwelling that are controlled by the modulated wind stress. To estimate effect of the ocean mean state to the EEIO SSTA in response to the anomalous wind stress, we also conducted additional experiment by only using the OGCM. This experiment could also reconfirm the seasonal sensitivity of the IO surface to the ocean dynamics corresponding to the surface wind anomalies. Identical wind stress anomalies are imposed to the climatological surface momentum flux in boreal summer (W-SR) and fall (W-FR) to drive the OGCM. To keep the experiment simple, the imposed anomalies are obtained from the average of the DC-SR and DC-FR. To account for the oceanic sensitivity to the initial conditions, a 10-member ensemble approach is

conducted. We also conduct the climatological flux run, which is driven by the monthly varying surface flux at the air-sea boundary. The climatology used here is obtained from the CGCM control run.

Figure 4 shows the imposed wind stress anomalies and composited SSTA after 3-months. The SSTA is difference between the run with imposed wind anomalies and the run with climatological wind stress. When the wind stress anomalies are inserted in the IO for the 3 months, both W-SR and W-FR reveal the Kelvin wave-like response along the thermocline (not shown). Due to the seasonal migration of the thermocline, the impacts on the SST variation for boreal summer reveal a significant cooling of the SST in the EEIO than those for the fall (Fig. 4a). The W-SR induces a significant cooling in the EEIO, with SSTA surpassing  $-0.8^{\circ}\text{C}$ . In contrast, the W-FR could not induce a significant cooling of the SST in the region (Fig. 4b), suggesting that the oceanic Kelvin wave response from boreal fall to winter does not contribute to the SSTA in the EEIO, because of the deeper thermocline. In addition to the atmospheric mean state, those of ocean at coastline of Sumatra during boreal summer are highly sensitive to the equatorial wind anomalies. Thus, both atmospheric and oceanic mean states in boreal summer drag in the strong coupled instability, which result in seasonally bound generation of the IOD at the following season.

#### 4. Conclusions

In general, the SST variability in the tropical IO is relatively small because of a strong radiative damping and thus there is need for the external forcing persistently (Li et al. 2003). Although both of dynamical and thermodynamical modulation in relation to the remote El Niño forcing contributes to the enhancement of the IOD and the BW, the IO SSTA mainly depends on the atmospheric mean state, namely monsoon circulation. As presented above, the IOD could be forced by various factors (e.g., Asian or Austral monsoon) through the wind modulation of the equatorial IO (e.g., Lau and Nath 2004). In addition to the recent studies, we also strengthen the role of the seasonal mean flow on air-sea feedback processes to understand the different response of the IO. Our approach to separate (season-slice) the seasonal impact of the El Niño on the IO strengthens the importance of the seasonality as mentioned above study.

In the World Climate Research Programme's (WCRP's) Coupled Model Intercomparison Project phase 3 (CMIP3: Meehl et al. 2007) data, many CGCMs failure to capture the generation of the IOD and BW (Saji et al. 2006). We are now comparing the relationship between the reproducibility of the SSTA and IO climatological state that could contribute to the more accurate simulation of the IO SSTA and their related tele-connections.

#### Acknowledgments

This work is supported by the Global Environment Research Fund (S-5-2) of the Ministry of the Environment, Japan. Drs. A. Kitoh, S. Yukimoto and O. Arakawa are acknowledged for providing the model source code. We express special thanks to Profs. R. Kawamura and T. Li for their helpful discussion and suggestions.

#### References

Allan, R. J., D. Chambers, W. Drosowsky, H. Hendon, M. Latif, N. Nicholls, I. Smith, R. C. Stone, and Y. Tourre, 2001: Is

- there an Indian Ocean dipole independent of the El Niño Southern Oscillations?, *CLIVAR Exchanges*, **6**, 18–22.
- Annamalai, H., R. Murtugudde, J. Potemra, S. P. Xie, P. Liu, and B. Wang, 2003: Coupled dynamics in the Indian Ocean: Spring initiation of the zonal mode, *Deep-Sea Res.*, **50B**, 2305–2330.
- Annamalai, H., S.-P. Xie, J. P. McCreary, and R. Murtugudde, 2005: Impact of Indian Ocean sea surface temperature on developing El Niño. *J. Climate*, **18**, 302–319.
- Horii, T., and K. Hanawa, 2004: A relationship between timing of El Niño onset and subsequent evolution. *Geophys. Res. Lett.*, **31**, L06304, doi:10.1029/2003/GL019239.
- Klein, S. A., B. J. Soden, and N. C. Lau, 1999: Remote sea surface temperature variations during ENSO: Evidence for a tropical atmospheric bridge. *J. Climate*, **12**, 917–932.
- Kug, J.-S., and I.-S. Kang, 2006: Interactive feedback between the Indian Ocean and ENSO. *J. Climate*, **19**, 1784–1801.
- Lau, N.-C., and M. J. Nath, 2004: Coupled GCM simulation of Atmosphere-Ocean variability associated with the zonally asymmetric SST changes in the Tropical Indian Ocean. *J. Climate*, **17**, 245–265.
- Li, T., B. Wang, C.-P. Chang, and Y. Zhang, 2003: A theory for the Indian Ocean dipole-zonal mode. *J. Atmos. Sci.*, **60**, 2119–2135.
- Li, T., Y. Zhang, E. Lu, and D. Wang, 2002: Relative role of dynamic and thermodynamic processes in the development of the Indian Ocean dipole: An OGCM diagnosis. *Geophys. Res. Lett.*, **29**, 2110, doi:10.1029/2002GL015789.
- Meehl, G. A., C. Covey, T. Delworth, M. Latif, B. McAvaney, J. F. B. Mitchell, R. J. Stouffer, and K. E. Taylor, 2007: The WCRP CMIP3 multimodel dataset: A new era in climate change research. *Bull. Amer. Meteor. Soc.*, **88**, 1383–1394.
- Murtugudde, R., and A. J. Busalacchi, 1999: Interannual variability of the dynamics and thermodynamics of the Tropical Indian Ocean. *J. Climate*, **12**, 2300–2326.
- Nagura, M., and M. Konda, 2005: The relationship between the interannual variation of the north Indian Ocean SST induced by surface wind and ENSO during Boreal Summer. *J. Climate*, **18**, 1942–1956.
- Ohba, M., and H. Ueda, 2007: An Impact of SST anomalies in the Indian Ocean in acceleration of the El Niño to La Niña transition. *J. Meteor. Soc. Japan*, **85**, 335–348.
- Saji, N. H., B. N. Goswami, P. N. Vinayachandran, and T. Yamagata, 1999: A dipole mode in the tropical Indian Ocean. *Nature*, **401**, 360–363.
- Saji, N. H., S.-P. Xie, and T. Yamagata, 2006: Tropical Indian Ocean variability in the IPCC 20th-century climate simulations. *J. Climate*, **19**, 4397–4417.
- Shinoda, T., M. A. Alexander, and H. H. Hendon, 2004: Remote response of the Indian Ocean to interannual SST variations in the tropical Pacific. *J. Climate*, **17**, 362–372.
- Smith, T. M., and R. W. Reynolds, 2004: Improved extended reconstruction of SST (1854–1997). *J. Climate*, **17**, 2466–2477.
- Ueda, H., and J. Matsumoto, 2000: A possible triggering process of east-west asymmetric anomalies over the Indian Ocean in relation to 1997/98 El Niño. *J. Meteor. Soc. Japan*, **78**, 803–818.
- Webster, P. J., A. Moore, J. Loschnigg, and R. Leben, 1999: Coupled ocean-atmosphere dynamics in the Indian Ocean during 1997–98. *Nature*, **401**, 356–360.
- Wyrtki, T., 1973: An equatorial jet in the Indian Ocean. *Science*, **181**, 262–264.
- Xie, S.-P., H. Annamalai, F. A. Schott, and J. P. McCreary, 2002: Structure and mechanisms of south Indian Ocean climate variability. *J. Climate*, **15**, 864–878.
- Yamagata, T., S. Behera, S. A. Rao, Z. Guan, K. Ashok, and N. H. Saji, 2003: Comments on “Dipoles, temperature gradients, and tropical climate anomalies.”, *Bull. Amer. Meteor. Soc.*, **84**, 1418–1422.
- Yukimoto, S., and Y. Kitamura, 2003: An investigation of the irregularity of El Niño in a coupled GCM. *J. Meteor. Soc. Japan*, **81**, 599–622.
- Yukimoto, S., A. Noda, A. Kitoh, M. Hosaka, H. Yoshimura, T. Uchiyama, K. Shibata, O. Arakawa, and S. Kusunoki, 2006: Present-Day climate and climate sensitivity in the Meteorological Research Institute Coupled GCM Version 2.3 (MRI-CGCM2.3). *J. Meteor. Soc. Japan*, **84**, 333–363.

Manuscript received 1 September 2009, accepted 12 November 2009  
 SOLA: <http://www.jstage.jst.go.jp/browse/sola/>